Functional characterization and comparison of intercellular communication in stem cell-derived cardiomyocytes.

Irene C. Marcu[1,2], Ardo Illaste[1], Pernilla Heuking[3], Marisa E. Jaconi[3], Nina D. Ullrich[1,2]

[1]Department of Physiology, University of Bern, Switzerland;
[2]Department of Physiology and Pathophysiology, University of Heidelberg, Germany;
[3]Department of Pathology and Immunology, University of Geneva, Switzerland.

Contact: Nina D. Ullrich
Department of Physiology and Pathophysiology
University of Heidelberg
Im Neuenheimer Feld 307, 4.OG
D-69120 Heidelberg
nina.ullrich@physiologie.uni-heidelberg.de

Running title: Coupling quality in SC-derived cardiomyocytes

Keywords: pluripotent stem cells, cardiomyocytes, electrophysiology, Ca^{2+} imaging, gap junctions

Authors contributions:
I.C.M.: Collection and assembly of data, data analysis and interpretation
A.I.: Data analysis and interpretation, manuscript writing
P.H.: Provision of study material, data interpretation
M.E.J.: Provision of study material, data collection and interpretation
N.D.U.: Conception and design, financial support, manuscript writing

Abstract

One novel treatment strategy for the diseased heart focuses on the use of pluripotent stem cell-derived cardiomyocytes (SC-CMs) to overcome the heart's innate deficiency for self-repair. However, targeted application of SC-CMs requires in-depth characterization of their true cardiogenic potential in terms of excitability and intercellular coupling at cellular level and in multi-cellular preparations. In this study, we elucidated the electrical characteristics of single SC-CMs and intercellular coupling quality of cell pairs, and concomitantly compared them with well-characterized murine native neonatal and immortalized HL-1 myocytes. *Firstly*, we investigated the electrical properties and Ca^{2+} signaling mechanisms specific to cardiac contraction in single SC-CMs. Despite heterogeneity of the new cardiac cell population, their electrophysiological activity and Ca^{2+} handling were similar to native cells. *Secondly*, we investigated the capability of paired SC-CMs to form an adequate subunit of a functional syncytium and analyzed gap junctions and signal transmission by dye transfer in cell pairs. We discovered significantly diminished coupling in SC-CMs compared to native cells, which could not be enhanced by a co-culture approach combining SC-CMs and primary CMs. Moreover, quantitative and structural analysis of gap junctions presented significantly reduced connexin expression levels compared with native CMs. Strong dependence of intercellular coupling on gap junction density was further confirmed by computational simulations. These novel findings demonstrate that despite the cardiogenic electrophysiological profile, SC-CMs present significant limitations in intercellular communication. Inadequate coupling may severely impair functional integration and signal transmission, which needs to be carefully considered for the prospective use of SC-CMs in cardiac repair.

Introduction

Recent advances in stem cell research fuel new hope for patients suffering from cardiovascular diseases. Especially for end stage heart failure (HF), classical therapies involving pharmacological interventions, surgical approaches like mechanical assist devices or even cardiac transplantations, can no longer support the ever growing number of HF patients. High prevalence of ischemic heart disease and parallel increase in global burden are calling for alternative treatment options, and stem cell-derived cardiomyocytes (SC-CMs) carry high potential for cell-based therapies of the diseased heart.

In vitro differentiation of pluripotent SCs into beating cardiomyocytes (CMs) was first achieved in 1981 [1-3] and since then, a new focus has emerged aiming at the development of the ideal cell type for replacing diseased myocardial tissue. Despite successful differentiation of SCs of different origin (embryonic – ESCs, or induced pluripotent – iPSCs) into spontaneously beating cell clusters with active cardiogenic marker genes, the resulting CMs present a fairly immature and highly variable cardiac phenotype [4]. In order to assess their true potential to replace and repair diseased myocardium [5], functional properties of these newly generated CMs need to be investigated with the necessary attention to details. In this regard, a placement of cell grafts of SC-CMs on affected myocardial tissue raises the question, whether these particular cells are capable of functional integration into the host myocardium and contribute actively to the electrical and mechanical activity of the cardiac tissue [6]. However, despite the efforts of previous studies to elucidate the electrical properties of SC-CMs and signal propagation in multicellular preparations [7, 8], a detailed and unequivocal characterization of the mechanisms that control contraction and cellular interactions of SC-CMs has not yet been provided [9-15].

In this original study, we investigated the electrical properties of single SC-CMs with regard to excitation-contraction (EC) coupling involving cardiac Ca^{2+} signaling mechanisms, and we characterized intercellular coupling quality at the level of cell pairs. In this context, it was of particular interest whether SC-CMs are able to establish intercellular contact sites by formation of gap junctions and communicate with each other in a manner similar to native CMs. Results from these experiments were directly compared with neonatal cardiac cells (NCMs) and with HL-1 cells, which represent well-characterized cardiac model systems of an immature cardiac phenotype [16]. Finally, we combined SC-CMs with native cardiomyocytes in a co-culture approach and evaluated the functional coupling between these mixed cell pairs. Our functional data were consolidated by structural analysis of the main cardiac gap junction proteins (i.e. connexins Cx43, Cx40, Cx45 and Cx30.2) and confirmed by computational simulations.

Our novel findings highlight a considerably impaired signal transmission between cell pairs when compared with native cardiomyocytes. These key findings contribute significantly to our growing understanding of the functional properties of SC-CMs and remind us of the challenges that

need to be overcome for future applications of these cells in clinical settings. *(Parts of these results have been presented in abstract form at scientific conferences.)*

Material and Methods

(*For a detailed description of the methods, see also Supporting Information.)*

Cardiac cell models

The murine CGR8 cell line (LGC Standards GmbH, Wesel, Germany) served as source of embryonic stem cells (ESCs). Differentiation into the cardiogenic lineage was adapted from a previously described protocol and achieved using the hanging drop method [17]. Single beating cells were obtained by mechanical and enzymatic dissociations of contractile areas within the embryoid bodies. Additionally, murine induced pluripotent stem cell-derived cardiomyocytes (iPSC-CMs, commercially available from Axiogenesis AG, Cologne, Germany) were used. For further comparison with native cardiomyocytes, mouse neonatal ventricular cardiomyocytes (NCMs) were kindly provided by Dr. Jan Kucera (University of Bern, Switzerland). Ventricular myocytes were obtained as previously described [18]. Experiments were approved by the State Veterinary Office of Bern, Switzerland, according to the Swiss Federal Animal Protection Law. An additional well-characterized cardiac cell model was used for our comparative study, namely the murine HL-1 cell line, directly obtained as a kind gift from Dr. William Claycomb [16]. All cells were kept at 37°C in a humidified incubator with 5% CO_2.

Electrophysiology

Cells were plated at low density on gelatin/fibronectin coated glass bottom dishes (MatTek Corporation). The patch-clamp technique was applied in the whole-cell mode controlled by an Axopatch 200B amplifier (Axon Instruments) and a custom-written acquisition software developed under LabView (National Instruments). Membrane currents were recorded in the voltage-clamp mode with a holding potential of -80 mV. Different test protocols were applied as indicated in the figures. Current-voltage relationships were determined, and specific test pulses were applied to activate I_{CaL} and to trigger Ca^{2+}-induced-Ca^{2+}release (CICR). Membrane currents were normalized to cell membrane capacitance. Spontaneous and triggered action potentials were recorded in the current-clamp mode. Alternatively, triggered action potentials were generated with a custom-built field stimulator at different stimulation frequencies at supra-threshold pulse amplitudes. Composition of internal and bath solutions are detailed in the supplemental information. Data were analyzed in IgorPro (WaveMetrics).

Confocal microscopy

Image acquisition was performed on a laser scanning confocal microscope (Microradiance, BioRad), which was paired with the patch-clamp setup and combined with electrophysiological

recordings. For confocal Ca^{2+} imaging, cells were loaded with the fluorescent Ca^{2+} indicator fluo-3 either via AM-ester loading of the cells (5 µM) or via single cell perfusion through the patch-clamp pipette using the water soluble salt K_5-fluo-3 (50 µmol/L), depending on the experimental setup. For dye-coupling experiments in cell pairs, the fluorescent gap junction permeant dye calcein was introduced into one cell of a cell pair using the patch clamp pipette. Time dependence of fluorescence increase was measured in the coupled cell. Fluorescent dyes were excited at 488 nm with an Argon ion laser and light emission was collected above 500 nm. Line-scan images were recorded at a rate of 500 lines/s. SR Ca^{2+} content was assessed with rapid pulses of 10 mmol/L caffeine, a ryanodine receptor agonist. Frame and line-scan images were analyzed in ImageJ (NIH) and further processed using IgorPro (WaveMetrics) or Canvas. Normalized fluorescence is indicated as F/F_0, and relative changes in fluorescence levels are shown as $\Delta F/F_0$. All measurements were performed at constant room temperature (22°C).

Immunocytochemistry

Cultured cells were grown on glass bottom dishes or glass coverslips and washed twice in PBS before and after fixation in 4% paraformaldehyde for 10 minutes. After permeabilization with 0.3% Triton-X, unspecific sites were blocked with 1% BSA in PBS for 30 minutes. Cells were stained for gap junctional Cx-43 protein (Chemicon), sarcolemmal L-type Ca^{2+} channels (Millipore), sarcoplasmic reticulum ryanodine receptors (Abcam) and sarcomeric α-actinin (Sigma-Aldrich). Primary and secondary antibodies were subsequently incubated for 2 hours at room temperature. For secondary antibodies, the respective primary antibody-specific Alexa Fluor 488 and 568 dyes were used (Lubio Science). Confocal images were taken with a laser scanning confocal microscope (Olympus FluoView1000).

RNA extraction and real-time PCR (qPCR)

Total RNA was extracted from cells with TRIZOL reagent (Invitrogen AG, Basel, Switzerland) according to the manufacturer's instructions. 2µg of total RNA was converted to cDNA with M-MLV Reverse Transcriptase (Invitrogen) using random primers in a 20µL reaction incubated at 25°C for 10 min followed by 50 min at 37°C and 15 min at 70°C (for primer information, see supplemental information). Volume was adjusted to 100µL. qPCR was performed with 20 ng of cDNA in a total volume of 25µL using SYBR green with the Biorad CFX96 Touch Real-time PCR Cycler (Bio-Rad Laboratories AG, Cressier, Switzerland) and at amplification temperatures of 60 and 62°C, according to the primer optimal amplification temperature. Using the $\Delta\Delta C_q$ method, analysis yielded relative gene expression value normalized to NCM expression levels. All reactions were run in triplicates. Data are expressed as mean±SEM normalized to control neonatal ventricular cardiomyocytes.

Diffusion model

Dye transfer between coupled cells was simulated with a one dimensional stochastic diffusion model. Each dye molecule undertook a random sized step at each time step Δt. Diffusion from one cell to the other was restricted by a semi-permeable barrier. A dye molecule coming in contact with the barrier during time step Δt had a probability p of crossing the barrier (and probability $1-p$ of bouncing back). Probability p is designated as the permeability of the barrier. After each time step, the concentration of dye molecules in a region similar to that used in the dye transfer experiment was recorded and, repeating this over many time steps, the dependence of dye concentration on time was obtained. In order to match the shape of this simulated dye transfer curve to experimentally obtained ones, only the permeability of the barrier was altered. The ratio of the optimal permeability values obtained for different cell types is indicative of the ratio of gap junction densities for the same cell types (e.g., $p_{NCM} / p_{HL1} = q$ means that gap junction density in NCMs is q times larger than in HL-1 cells, [19]).

Statistical analysis

Data are presented as mean±SEM. Statistical significance was evaluated by either Student's t-test or one-way ANOVA test. A *P*-value below 0.05 was considered to indicate significant difference between samples.

Results

1. Electrophysiological characterization of SC-CMs

For an initial functional characterization of the successful cardiogenic differentiation of SC-CMs, electrical excitability, spontaneous beating behavior, and the presence of characteristic cardiac ion channels were tested. In general, two types of cells with cardiogenic properties could be distinguished: spontaneously contractile cells (Fig. 1A) and cells with no intrinsic contractile activity but electrical excitability as recognized by electrical field stimulation or patch clamp analysis (Fig. 1B). The action potential (AP) frequency of spontaneously beating cells was within a similar range as from freshly isolated neonatal cardiomyocytes (NCMs) and HL-1 cells and amounted to 0.87±0.1 Hz, 0.74±0.2 Hz and 0.78±0.02 Hz in SC-CMs, NCMs and HL-1 cells, respectively (Fig. 1C). Fig. 1D shows evoked APs in response to different stimulation frequencies in current clamp mode.

Given the fact that a fraction of SC-CMs was not spontaneously beating but excitable by electrical stimulation, we tested their electrical excitability under voltage-clamped conditions. With regard to adult cardiomyocytes, which under resting conditions are also not spontaneously contracting, we tested the hypothesis, that on a functional level, silent SC-CMs may correspond to the electrical phenotype of adult cardiomyocytes, resulting in the observed AP shape analogous to

the AP of a ventricular myocyte (see above, Fig. 1B, 1D). Using the whole-cell mode of the patch-clamp technique, we first tested SC-CMs for the presence of the fast voltage-dependent Na^+ current, which produces the sharp upstroke of the AP in adult cardiomyocytes. Stimulation of the voltage-dependent Na^+ channel revealed fast activating and inactivating inward Na^+ currents with the characteristic steep current-voltage (I-V) relationship peaking around -40 mV (Fig. 2A). Currents were rapidly and reversibly inhibited by addition of tetracaine (1 mmol/L), a local anesthetic drug and inner pore blocker of Na^+ channels [20].

Then we looked for the presence of the main Ca^{2+} channel that is responsible for the primary phase of the excitation-contraction (EC)-coupling mechanism, the L-type Ca^{2+} channel. Depolarization of the sarcolemma activates this voltage-dependent Ca^{2+} channel leading to Ca^{2+} influx into the cell, which serves as a trigger for Ca^{2+}-induced Ca^{2+} release and the initiation of contraction. In SC-CMs, nifedipine-sensitive L-type Ca^{2+} currents (10 µmol/L) were recorded and showed their characteristic slow activation and inactivation kinetics with peak current amplitudes around +5 mV in the I-V curve (Fig. 2B).

Despite the low presence of T-type Ca^{2+} channels in adult ventricular myocytes, cardiomyocytes from a premature developmental stage show large T-type Ca^{2+} currents (NCMs, HL-1 cells), which has previously been associated with the proliferative potential of pluripotent stem cells, developing and cancer cells [21-24]. Besides their cardiac function and role as a voltage-dependent ion channel, T-type Ca^{2+} channels may also be involved in regulatory mechanisms of basic cellular functions such as cell cycle control and gene expression by modulation of the cytosolic Ca^{2+} concentration [21, 25]. We therefore tested SC-CMs for T-type Ca^{2+} currents and described rapidly activating and inactivating currents, which were reversibly inhibited by mibefradil (5 µmol/L, Fig. 2C). Maximal current amplitudes were measured at -30 mV. I-V curves of the ionic currents and their selective inhibition are summarized in Fig. 2.

2. Ca^{2+} signals and EC-coupling in SC-CMs

Since at the functional level, SC-CMs correspond to an early cardiac phenotype, the mechanism underlying contraction in these cells has been questioned [11, 14, 26]. In particular, previous characterizations showed ambiguous results in terms of the source of Ca^{2+} for contraction and the maturity of the SR [10, 14, 15, 27]. Here, we investigated the EC-coupling mechanism in SC-CMs at a structural and functional level. Fig. 3A illustrates the expression pattern of the major Ca^{2+}-handling EC-coupling proteins, namely the L-type Ca^{2+} channel and the ryanodine receptor (RyR2, the SR Ca^{2+} release channel). Parallel immunostaining of the sarcomeric protein α-actinin indicates myofilament orientation and the position of the Z-line. Electrical stimulation of the L-type Ca^{2+} channel in patch-clamped SC-CMs triggered Ca^{2+} release from the SR (Fig. 3). Sample traces for I_{CaL}, line-scan images and corresponding line profiles are given in Fig. 3B. Currents and responding Ca^{2+} transients were sensitive to ß-adrenergic stimulation with isoproterenol (Iso, 1 µmol/L), leading to elevated diastolic Ca^{2+} levels, increased peak I_{CaL} and Ca^{2+} transient

amplitudes. Quantitative characterization of changes in I_{CaL} and Ca^{2+} transients before (Ctrl) and during ß-adrenergic stimulation are summarized in Fig. 3C. Despite significant increase in both I_{CaL} and Ca^{2+} transient peak amplitudes, time to peak (TTP; 135±33 and 124±37 ms, respectively), full duration at half maximum amplitude (FDHM; 482±52 and 526±49 ms, respectively) and the time constant of Ca^{2+} transient decay (τ; 388±□□ □□□ □□□□□□ □□□ □□□□□□□□□□□□) were not significantly enhanced during ß-adrenergic stimulation ($n_{Control}$=20, n_{Iso}=13 cells). Caffeine-induced Ca^{2+} release from the SR was compared with native and HL-1 cardiomyocytes and amounted to similar values in all groups (Fig. 3D), indicative of a functional SR Ca^{2+} store in SC-CMs.

3. Intercellular coupling of cell pairs

For the anticipated therapeutic use of SC-CMs in diseased myocardium, these cells need to integrate and connect with host myocardial cells in order to participate in electrical signal transmission forming a functional syncytium with similar properties as native cardiomyocytes [28]. In order to investigate the capability of SC-CMs for intercellular coupling, we studied electrical coupling in cell pairs. Assuming connection of these cells via gap junctions, we hypothesized that depolarization-induced CICR of one cell will also lead to CICR in the neighbored cell via Ca^{2+} transport through gap junctions and further RyR2-mediated Ca^{2+} release. We electrically stimulated Cell 1 of a cell pair via the patch-clamp pipette and recorded Ca^{2+} transients using confocal imaging of fluo-3 in both cells. Fig. 4 illustrates the experimental setup. A line-scan is fitted through both cells. Depolarization of Cell 1 activated the L-type Ca^{2+} channel leading to Ca^{2+} influx, which triggered CICR via RyR2 in both adjacent cells as shown in the line-scan image and the corresponding line-profiles. Ca^{2+} release in Cell 2 occurred without any temporal delay indicating functional coupling between both cells via Ca^{2+} transmission between the two cytosolic compartments of both cells.

4. Metabolic coupling in identical cells and mixed cell pairs

To further investigate gap junction-mediated signal transmission, we studied the quality of metabolic coupling using the method of dye transfer [29]. Calcein, a gap junction-permeant fluorescent dye, was introduced into Cell 1 of a cell pair, and time-dependence of dye transfer was assessed by measuring the increase in fluorescence in Cell 2. For comparison between different cell pairs, fluorescence was normalized to the contact length between both cells. Fig. 5A illustrates a time-series of dye transfer in X-Y images of a cell pair. Time-dependence of dye transfer in SC-CMs was compared to native neonatal cardiomyocytes and cardiac HL-1 cells (Fig. 5B). While neonatal cardiomyocytes show a fast increase in fluorescence in the neighbored cell, dye transfer was significantly slower in both SC-CMs and HL-1 cells, the latter being known for relatively low connectivity [30-32]. Curves were fitted with a sigmoidal function according to the expected temporal kinetics of particle diffusion between two compartments (see below). Dye diffusion through gap junctions was reversibly inhibited by heptanol (1 mmol/L), a non-specific gap junction

uncoupler [33]. Sample traces shown in Fig. 5C illustrate the rapid rise in calcein-emitted fluorescence in Cell 1, while during heptanol application and functional uncoupling, no dye was transmitted to Cell 2. Only after washout of heptanol, calcein could diffuse again thereby slowly increasing fluorescence in Cell 2. Relative intensity of fluorescence at 120 sec of dye coupling was compared in all tested cell types and is summarized in Fig. 5D.

In an additional set of experiments, we tested intercellular coupling in iPSC-derived cardiomyocytes using the same experimental setup of dye-coupling with calcein. Interestingly, iPSC-CMs showed the same temporal diffusion dynamics as SC-CMs in cell pairs, confirming our findings of significantly reduced coupling between SC-CMs compared to native cardiomyocytes (red trace in Fig. 5E).

In order to mimic the setting of a host-graft cell pair, we were interested in the intercellular coupling quality of mixed cell pairs. We hypothesized that co-culture of SC-CMs with native cardiomyocytes, which exhibit strong intercellular coupling, may enhance the formation of gap junctions between this heterogeneous cell pair. For this purpose, iPSC-CMs expressing a genetically encoded fluorescent reporter (GFP) were paired with native NCMs (or *vice versa,* normal iPSC-CMs coupled with GFP-labeled NCMs), and dye coupling in both directions was assessed as described above. Our results show that dye transfer is not enhanced in mixed cell pairs, thus, co-culture of SC-CMs with NCMs did not increase the formation of functional gap junctions between both cells (blue trace in Fig. 5E). Normalized calcein fluorescence in Cell 2 of pure iPSC-CMs and mixed cell pairs at 120 s of dye coupling are summarized in Fig. 5F (data of NCMs are replicates of Fig. 5D).

5. Comparative analysis of connexin expression

Since the predominant intercellular gap junction channels in the heart are composed of Cx43 subunits, we investigated the expression pattern of Cx43 in SC-CMs. Cx43-positive clusters were identified at intercellular contact sites in SC-CMs and compared with NCMs, HL-1 and iPSC-CMs (Fig. 6A) in a qualitative way. NCMs exhibited strongest membrane expression of Cx43, while in ESC-, iPSC-CMs and HL-1 cells, expression was moderate with a punctate pattern at cell-to-cell contact sites. This difference in Cx43 expression between SC-CMs and NCMs was further confirmed at mRNA level by quantitative PCR assays. NCMs demonstrated highest expression levels of Cx43 mRNA, while Cx43 expression in all three other cell types was very low. Expression levels of Cx43 in SC-CMs, iPSC-CMs and HL-1 cells relative to NCMs are shown in Fig. 6B. These results confirm a significant difference in Cx43 expression between native NCMs and newly generated SC-CMs (even of different origin) and may underlie the structural differences of intercellular channel formation at cell-to-cell contact sites seen in the immunostainings (Fig. 6A).

In addition, we investigated expression levels of other cardiac connexins, namely Cx30.2, Cx40 and Cx45, in order to reveal their possible contribution to signal transmission in SC-CMs. Since these connexins are selectively relevant for tissue specific signal transmission in the heart

(ventricle: Cx43; atria: Cx40 and Cx43; conductive system: Cx45, but also Cx30.2, Cx40 and Cx43), differential expression pattern relative to NCMs may reveal the contribution, if substantial, of a specific cardiac type within SC-CMs. In all tested cell types, connexin expression levels were lower than in NCMs. Especially, Cx40 showed overall significantly lower expression levels in the tested cells. From these data however, we cannot not conclude on any specific type of cardiomyocytes, but rather accept that the connexin expression pattern in SC-CMs is different from native cardiomyocytes. Expression results for all four connexins are summarized in Suppl. Fig. 1.

6. Dye-Transfer Diffusion Model

The low connexin gene expression in SC-CMs and the reduced formation of intercellular channels at the structural level strongly consolidate our functional data, suggesting that the temporal profile of metabolite transfer between two cells directly depends on the number of available intercellular connections. We have synthesized the relationship of these parameters and created a model, which reflects the kinetics of dye transfer as a function of the number of established gap junctions.

The temporal dynamics of dye transfer from one cell to the other followed a sigmoidal function and can be approximated by a simple diffusion model as explained in detail in the methods section. In short, dye transfer through gap junctions is simulated as diffusion through a semi-permeable barrier. In order to obtain fits for experimental dye transfer curves, only the permeability of the barrier was altered (Fig. 7A). Experimental data could be reproduced when the permeability of the barrier for NCMs was ~6 times greater than for all other cell types. This is equivalent to a 6–fold difference in gap junction density (Fig. 7B; experimental data are replicates of Fig. 5) and strongly correlates with our quantitative assessment of Cx43 expression levels.

Discussion

The present study provides a direct functional characterization and comparison of the electrical properties and intercellular communication of stem cell-derived cardiomyocytes relative to well-known primary neonatal and immortalized HL-1 CMs. Using a combination of the patch clamp technique and confocal imaging, we describe important similarities between SC-CMs and native CMs, which underline their potential to serve as cell grafts for replacement of diseased myocardial cells. However, we discovered for the first time substantial functional differences between the newly developed cardiomyocytes and native cardiac cells, which severely impair intercellular communication between neighbored cells, a crucial requirement of cardiomyocytes for intact signal propagation across the myocardium. Impact and possible consequences of our original findings are discussed below.

Characterization of the cardiogenic phenotype

In this study, we worked with mouse embryonic stem cells, which represent a gold standard for deriving *bona fide* cardiomyocytes, as well as induced pluripotent SC-CMs. Due to their pluripotency, experiments with ESCs provide insight into the feasibility and best possible achievements that can be expected with newly developed cardiac cells. The strong advantage of using ESCs as source for novel cardiomyocytes clearly lies in their young age and purity without any epigenetic history. However, ethical issues and availability of ESCs in terms of clinical grade and HLA-matching undoubtedly limit future clinical applications. iPSCs provide an excellent alternative for the use of stem cells in cell therapy, yet many questions remain to be answered including late consequences of phenotype switch and change in cell fate, age and epigenetic memory of these cells [34]. Direct functional comparison of these cells with true ESC-derived cardiomyocytes is needed in order to uncover possible significant differences or even to emphasize and prove the similarities between iPSC- and ESC-CMs.

Spontaneous cardiac differentiation of ESCs using the hanging drop method resulted in beating cell clusters comprising a heterogeneous population of early premature cardiac myocytes. Due to the fact that different ESC lines and differentiation protocols may lead to strong phenotype variability, detailed characterization is essential to allow comparison with previous reports on SC-CMs. Here, we provide experimental evidence that ESC-CMs *i*) present all basic functional characteristics (typical for cardiomyocytes) at the electrophysiological level, *ii*) respond to humoral stimuli, and *iii*) display a functional SR Ca^{2+} store needed for efficient Ca^{2+}-induced Ca^{2+}-release-based excitation-contraction coupling. Working with a murine system allowed a direct comparison with native cardiomyocytes derived from neonatal mice and immortalized murine cardiac HL-1 cells. Both cell types are very well characterized cardiac cell systems providing cardiomyocytes of an immature or early cardiac phenotype [4, 16, 35]. Therefore, they are optimal control cells for our study.

Classification of immature and spontaneously active SC-CMs upon their functional characteristics is difficult and highly debated. The most reliable distinctive criterion might be the shape and temporal characteristics of the action potential displayed by a particular cell. Even then, ambiguities may remain, which render a clear categorization almost impossible. From the differences in activity, we distinguished spontaneously active cells (pacemaker-type) from cells that were silent at rest but electrically excitable (working myocardial cell type). As confirmation of the cardiac phenotype, cells responded to different pacing frequencies and exhibited cardiac ion channels relevant for EC-coupling. Frequency of spontaneous APs was in line with neonatal and HL-1 cardiomyocytes.

Spontaneous activity in cardiomyocytes is often regarded as sign for immaturity as in pre-/neonatal cells. Accordingly, lack of intrinsic beating activity may be indicative for a step towards myocyte maturation. Therefore, heterogeneity in the cell population may be interpreted as a mixture of cardiac cells in different developmental stages. Consequently, a time-dependent

increase in maturation over culture time might be expected, as it has been described by previous studies [36]. However, within the time window of our experiments, which was up to 14 days post dissociation, no tendency towards a shift in the ratio of beating to silent cells was observed. In addition, contractile cells temporally co-existed with silent ones from day 1 post dissociation, which favors the conclusion that cells of different cardiac phenotypes resulted in parallel during spontaneous cardiac differentiation.

Quality of EC-coupling and sympathetic response

Structural and functional assessment of the EC-coupling machinery revealed expression of the respective Ca^{2+} channels required for Ca^{2+}-induced-Ca^{2+} release (CICR), the functional basis underlying each contraction. L-type Ca^{2+} channels are highly abundant and produce similar current densities as described for other native CMs [37-39]. Membrane depolarization leads to Ca^{2+} influx via L-type Ca^{2+} channels, which activates RyR2 at the sarcoplasmic reticulum membrane leading to a large cytosolic Ca^{2+} signal and initiating contraction [40]. Therefore, unlike previous findings [14], contraction depends on SR Ca^{2+} release rather than trans-sarcolemmal Ca^{2+} influx.

Both, membrane I_{CaL} and Ca^{2+} transients are enhanced during ß-adrenergic stimulation, indicating a functional receptor system and intracellular signaling cascade responsive to one of the most critical sympathetic modulator of the heart. However, enhanced inotropy is not accompanied by increased lusitropy, as seen in the temporal profile of Ca^{2+} transients. While in adult CMs, ß-adrenergic stimulation also speeds up relaxation by reducing Ca^{2+} transient duration and enhancing Ca^{2+} removal mechanisms, a statistically valid increase in lusitropy has not been detected in SC-CMs. Furthermore, time-to-peak (TTP) was not enhanced in SC-CMs. In contrast to adult CMs, where ß-adrenergic stimulation leads to improved Ca^{2+} release synchronization [41, 42] by enhancing availability of Ca^{2+} release units upon stimulation and by shortening TTP, a similar effect was not observed here. A possible explanation for the lack of synchronization may lie in the different micro-architecture of immature CMs, which are devoid of any transverse (t-)tubular system and, thus, bereft of the structural basis for a spatially and temporally optimized amplification of the initial Ca^{2+} influx derived from I_{CaL}. Interestingly, despite the lack of a t-tubular network in SC-CMs (and other immature CMs), L-type Ca^{2+} channels show a regular and striated expression pattern at the sarcolemma, which reminds of the expression pattern of L-type Ca^{2+} channels along the t-tubular membrane invaginations in adult cells. Therefore, it may be thinkable that a structural pre-disposition recruits L-type Ca^{2+} channels along the future sites of t-tubular membrane invaginations. However, this assumption can only be verified if induction of t-tubules can be achieved in cultured cardiomyocytes, an experimental challenge, which remains to be realized.

Intercellular communication by electrical stimulation and dye transfer

SC-CMs offer an excellent experimental model to study many cardiac diseases, especially

those related to ion channel mutations (e.g. [43-45]), as they present the same disease phenotype as adult cardiac cells. Still, the ultimate goal of SC-based research is to provide appropriate cells for replacement of diseased myocardium after injury (e.g. myocardial infarction). To achieve this aim, several functional requirements for the new CMs need to be met. It is not enough that the single cell as building block of cardiac tissue provides the same functional complexity of an adult CM, the new cells also need to integrate into the host myocardium and connect with their immediate neighbors in order to participate in signal propagation.

In this study, we investigated the intercellular coupling properties of SC-CMs at the level of cell pairs and directly compared their properties with primary and immortalized cardiac cells. According to our initial hypothesis, we tested the idea that SC-CMs couple to each other like neonatal CMs do. Our first approach for this investigation was based on electrical stimulation of one cell of a pair to induce CICR in the same cell, and via Ca^{2+}-diffusion through gap junctions, we anticipated the occurrence of Ca^{2+}-dependent RyR2 activation (CICR) in the cell neighbor as well. This was indeed the case as shown in Fig. 4, as electrical stimulation of one patch-clamped cell leads to temporally synchronized CICR in both cells. However, since a membrane-delimited and gap junction-independent stimulation of the attached cell remains a possibility for CICR activation in Cell 2, we applied a different approach. Using the fluorescent properties of the gap junction-permeant dye calcein, we quantified the time dependence of dye transfer from one cell to the other via gap junctions. We discovered a striking difference in the temporal pattern of dye transfer in SC-CMs, which was significantly slower when compared with neonatal CMs. Interestingly, calcein permeation in SC-CM pairs was similar as in HL-1 cell pairs, previously reported to display low intercellular coupling attributed to low Cx43 expression [31, 46]. The differences in coupling were very pronounced and reliably repeatable, which is also reflected in the statistical analysis.

In a recent study, functional integration and survival of grafted hESC-CMs into non-human primate hearts was presented over a three month period post cell transplantation [5]. However, the study also clearly reported in all hearts receiving hESC-CMs the detection of arrhythmias including premature ventricular contractions and runs of ventricular tachycardia, possibly due to re-entrant circuits or graft automaticity, but the underlying mechanism was not identified. Our study investigated exactly this phenomenon, namely the coupling properties of SC-CMs with each other and, importantly, with native NCMs – an experimental setting for functional integration in the 2-cell configuration, in which cell-to-cell coupling can be at best investigated. Presenting several lines of evidence, our results indicate a significant reduction in intercellular coupling efficiency of SC-CMs (ESC and iPSC-derived) with each other and with native cardiomyocytes due to very low expression of gap junction connexins. This finding may likely account for the pro-arrhythmic behavior of such cell grafts *in vivo*. Indeed, deficient intercellular coupling at the border between host and grafted cells may slow down electrical signal transmission across the border and through the cell graft, thereby producing inhomogeneous excitation patterns favoring re-entry circuits and isolated contractions or, even worse, creating a conduction barrier, especially at higher pacing

rates.

Of note, we uncovered prominent disparities in the expression of Cx43, the main cardiac gap junction protein, both at the protein and mRNA levels between SC-CMs and native NCMs, thus confirming the original functional findings. Other tested connexins also revealed reduced expression levels compared to NCMs. However, due to the rather insignificant expression levels of those connexins in NCMs, their even lower expression in SC-CMs is almost negligible for any functional implications [28, 47]. We also found the same significant difference in dye transfer kinetics and connexin expression when testing another source of SC-CMs, the iPSC-CMs. A recent study by Prudat Y *et al.* [48] demonstrated the importance of Cx43 expression levels in the context of conduction velocity and conduction block across strands of primary fetal ventricular myocytes presenting different Cx43 levels. These data are in line with our findings, namely that intercellular communication in mixed cardiac cell populations is mainly limited by Cx43 levels. Therefore, our data strongly support the notion that intercellular coupling via gap junctions is severely impaired in SC-CMs in comparison with primary NCMs and could not simply be rescued *in vitro* using a co-culture approach of mixed cell pairs consisting of SC-CMs and NCMs. Therefore, we conclude that low coupling is an intrinsic property of SC-CMs (and of HL-1 cells as well) irrespective of their assumed cardiac sub-phenotype. With this new knowledge, future *in vivo* experiments should focus on the deficiencies of these cells by trying to improve intercellular coupling and signal transmission across grafted cell patches.

In summary, we show that reduced intercellular communication results from reduced presence of gap junctions. Using a computational model of restricted diffusion, we were able to reproduce experimentally obtained temporal kinetics of dye transfer by modulating the density of gap junction channels along the contact surface of the coupled cell pair. As we were only interested in relative changes in intercellular coupling, a simple stochastic model was sufficient and the use of a more complicated model was unwarranted [29]. Our model indicates a ~6 fold reduction in gap junction density in all studied cell types when compared to NCMs. As, in essence, gap junction density determines the overall resistivity of intercellular couplings, which is continuously related to AP conduction velocity [49], this latter is consequently expected to considerably decrease at tissue level for the studied cardiac cell types other than NCMs.

Our findings have a potentially great impact on the future use of SC-CMs for cell grafts in diseased hearts, since strongly impaired intercellular coupling may result in a significant conduction barrier limiting signal propagation across the myocardium [48]. The functional consequence of such reduced signal transmission properties may express in form of arrhythmogenic hot spots at the site of cell grafts and may therefore lead to severe disturbances of the electrical activity of the heart. Our data clearly show that the electrical properties of single SC-CMs, as well as the processing of modulatory endocrine stimuli that resemble that of of native

CMs, are not sufficient to reproduce the same functional complexity, which will operate in a multifaceted three-dimensional environment as the real heart. Therefore, careful investigations are required to improve the coupling quality of SC-CMs in multi-cellular preparations for clinical use.

Acknowledgements

We wish to thank Drs. Ernst Niggli, Miguel Fernandez and Tamara Horn for stimulating discussions. We thank Dr. William Claycomb (Department of Biochemistry and Molecular Biology, LSU School of Medicine, New Orleans, USA) for his kind gift of the HL-1 cell line, and the group of Dr. Jan Kucera (Department of Physiology, University of Bern) for sharing neonatal cardiomyocytes with us. Many thanks to Helene Hinnen and Sabine Schneider, as well as Stefano Jaconi (MEJ group) for their expert technical assistance. This work was supported by the Ambizione grant of the Swiss National Science Foundation (PZ00P3_131987 to N.D.U.).

References

1. Evans M. Discovering pluripotency: 30 years of mouse embryonic stem cells. **NAT REV MOL CELL BIOL** 2011;12(10):680–686.

2. Martin GR. Isolation of a pluripotent cell line from early mouse embryos cultured in medium conditioned by teratocarcinoma stem cells. **PROC NATL ACAD SCI USA** 1981;78(12):7634–7638.

3. Evans MJ, Kaufman MH. Establishment in culture of pluripotential cells from mouse embryos. **NATURE** 1981;292(5819):154–156.

4. Harding SE, Ali NN, Brito-Martins M, et al. The human embryonic stem cell-derived cardiomyocyte as a pharmacological model. **PHARMACOLOGY & THERAPEUTICS** 2007;113(2):341–353.

5. Chong JJH, Yang X, Don CW, et al. Human embryonic-stem-cell-derived cardiomyocytes regenerate non-human primate hearts. **NATURE** 2014;510(7504):273–277.

6. Xue T, Cho HC, Akar FG, et al. Functional integration of electrically active cardiac derivatives from genetically engineered human embryonic stem cells with quiescent recipient ventricular cardiomyocytes: insights into the development of cell-based pacemakers. **CIRCULATION** 2005;111(1):11–20.

7. Hescheler J, Halbach M, Egert U, et al. Determination of electrical properties of ES cell-derived cardiomyocytes using MEAs. **J. ELECTROCARD.** 2004;37:110–116.

8. Nussinovitch U, Shinnawi R, Gepstein L. Modulation of cardiac tissue electrophysiological properties with light-sensitive proteins. **CARDIOVASC RES** 2014;102(1):176–187.

9. Li Sen, Cheng H, Tomaselli GF, et al. Mechanistic basis of excitation-contraction coupling in human pluripotent stem cell-derived ventricular cardiomyocytes revealed by Ca^{2+} spark characteristics - direct evidence of functional Ca^{2+}-induced Ca^{2+} release. **HRTHM** 2014;11(1):133–140.

10. Fu J-D, Jiang P, Rushing S, et al. Na^{+}/Ca^{2+} exchanger is a determinant of excitation–contraction coupling in human embryonic stem cell–derived ventricular cardiomyocytes. **STEM CELLS DEV** 2010;19(6):773–782.

11. Zhu W-Z, Santana LF, Laflamme MA. Local control of excitation-contraction coupling in human embryonic stem cell-derived cardiomyocytes. Schwartz A, ed. **PLOS ONE** 2009;4(4):e5407.

12. Satin J, Itzhaki I, Rapoport S, et al. Calcium handling in human embryonic stem cell-derived cardiomyocytes. **STEM CELLS** 2008;26(8):1961–1972.

13. Kapur N, Banach K. Inositol-1,4,5-trisphosphate-mediated spontaneous activity in mouse embryonic stem cell-derived cardiomyocytes. **J. PHYSIOL. (LOND.)** 2007;581(3):1113–1127.

14. Dolnikov K, Shilkrut M, Zeevi-Levin N, et al. Functional properties of human embryonic stem cell-derived cardiomyocytes: intracellular Ca^{2+} handling and the role of sarcoplasmic reticulum in the contraction. **STEM CELLS** 2006;24(2):236–245.

15. Fu JD. Crucial role of the sarcoplasmic reticulum in the developmental regulation of Ca^{2+} transients and contraction in cardiomyocytes derived from embryonic stem cells. **FASEB J** 2005.

16. Claycomb WC, Lanson NA, Stallworth BS, et al. HL-1 cells: a cardiac muscle cell line that contracts and retains phenotypic characteristics of the adult cardiomyocyte. **PROC NATL ACAD SCI USA** 1998;95(6):2979–2984.

17. Meyer N, Jaconi M, Landopoulou A, et al. A fluorescent reporter gene as a marker for ventricular specification in ES-derived cardiac cells. **FEBS LETTERS** 2000;478(1-2):151–158.

18. Thomas SP, Kucera JP, Bircher-Lehmann L, et al. Impulse propagation in synthetic strands of neonatal cardiac myocytes with genetically reduced levels of connexin43. **CIRC. RES.** 2003;92(11):1209–1216.

19. Illaste A, Laasmaa M, Peterson P, et al. Analysis of molecular movement reveals latticelike obstructions to diffusion in heart muscle cells. **BIOPHYSJ** 2012;102(4):739–748.

20. Bruhova I, Tikhonov DB, Zhorov BS. Access and binding of local anesthetics in the closed sodium channel. **MOL. PHARM.** 2008;74(4):1033–1045.

21. Rodriguez-Gomez JA, Levitsky KL, Lopez-Barneo J. T-type Ca^{2+} channels in mouse embryonic stem cells: modulation during cell cycle and contribution to self-renewal. **AJP: CELL PHYSIOL.** 2012;302(3):C494–C504.

22. Capiod T. Cell proliferation, calcium influx and calcium channels. **BIOCHIMIE** 2011;93(12): 2075–2079.

23. Lory P, Bidaud I, Chemin J. T-type calcium channels in differentiation and proliferation. **CELL CALCIUM** 2006;40(2):135–146.

24. Huc S, Monteil A, Bidaud I, et al. Regulation of T-type calcium channels: Signalling pathways and functional implications. **BBA - MOL. CELL RES.** 2009;1793(6):947–952.

25. Vassort G, Talavera K, Alvarez J. Role of T-type Ca^{2+} channels in the heart. **CELL CALCIUM** 2006;40(2):205–220.

26. Mauritz C, Schwanke K, Reppel M, et al. Generation of functional murine cardiac myocytes from induced pluripotent stem cells. **CIRCULATION** 2008;118(5):507–517.

27. Liu J, Fu J-D, Siu C-W, et al. Functional sarcoplasmic reticulum for calcium handling of human embryonic stem cell-derived cardiomyocytes: insights for driven maturation. **STEM CELLS** 2007;25(12):3038–3044.

28. Desplantez T, Dupont E, Severs NJ, et al. Gap junction channels and cardiac impulse propagation. **J. MEMBR. BIOL.** 2007;218(1-3):13–28.

29. Eckert R. Gap-junctional single-channel permeability for fluorescent tracers in mammalian cell cultures. **BIOPHYSJ** 2006;91(2):565–579.

30. Mureli S, Gans CP, Bare DJ, et al. Mesenchymal stem cells improve cardiac conduction by upregulation of connexin 43 through paracrine signaling. **AJP: HEART CIRC. PHYSIOL.** 2013;304(4):H600–H609.

31. Dias P, Desplantez T, El-Harasis MA, et al. Characterisation of connexin expression and electrophysiological properties in stable clones of the HL-1 myocyte cell line. Barnes S, ed. **PLOS ONE** 2014;9(2):e90266.

32. McCain ML, Desplantez T, Geisse NA, et al. Cell-to-cell coupling in engineered pairs of rat ventricular cardiomyocytes: relation between Cx43 immunofluorescence and intercellular electrical conductance. **AJP: HEART CIRC. PHYSIOL.** 2012;302(2):H443–50.

33. Takens-Kwak BR, Jongsma HJ, Rook MB, et al. Mechanism of heptanol-induced uncoupling of cardiac gap junctions: a perforated patch-clamp study. **AJP: CELL PHYSIOL.** 2002;262(31):C1531–8.

34. Yoshida Y, Yamanaka S. iPS cells: A source of cardiac regeneration. **J MOL CELL CARDIOL** 2011;50(2):327–332.

35. White SM, Constantin PE, Claycomb WC. Cardiac physiology at the cellular level: use of cultured HL-1 cardiomyocytes for studies of cardiac muscle cell structure and function. **AJP: HEART CIRC. PHYSIOL.** 2004;286(3):H823–9.

36. Sartiani L, Bettiol E, Stillitano F, et al. Developmental changes in cardiomyocytes differentiated from human embryonic stem cells: a molecular and electrophysiological approach. **STEM CELLS** 2007;25(5):1136–1144.

37. Alden KJ, Goldspink PH, Ruch SW, et al. Enhancement of L-type Ca^{2+} current from neonatal mouse ventricular myocytes by constitutively active PKC-beta II. **AJP: CELL PHYSIOL.** 2001;282(4):C768–C774.

38. Xiao YF. Enhancement of cardiac L-type Ca^{2+} currents in transgenic mice with cardiac-specific overexpression of CYP2J2. **MOL. PHARM.** 2004;66(6):1607–1616.

39. Ullrich ND, Fanchaouy M, Gusev K, et al. Hypersensitivity of excitation-contraction coupling in dystrophic cardiomyocytes. **AJP: HEART CIRC. PHYSIOL.** 2009;297(6):H1992–H2003.

40. Bers DM. Cardiac excitation-contraction coupling. **NATURE** 2002;415(6868):198–205.

41. Ogrodnik J, Niggli E. Increased Ca^{2+} leak and spatiotemporal coherence of Ca^{2+} release in cardiomyocytes during beta-adrenergic stimulation. **J. PHYSIOL. (LOND.)** 2010;588(Pt 1):225–242.

42. Ullrich ND, Valdivia HH, Niggli E. PKA phosphorylation of cardiac ryanodine receptor modulates SR luminal Ca^{2+} sensitivity. **J MOL CELL CARDIOL** 2012;53(1):33–42.

43. Itzhaki I, Maizels L, Huber I, et al. Modelling the long QT syndrome with induced pluripotent stem cells. **NATURE** 2011;471(7337):225–229.

44. Zhang XH, Haviland S, Wei H, et al. Ca^{2+} signaling in human induced pluripotent stem cell-derived cardiomyocytes (iPS-CM) from normal and catecholaminergic polymorphic ventricular tachycardia (CPVT)-afflicted subjects. **CELL CALCIUM** 2013;54(2):57–70.

45. Knollmann BC. Induced pluripotent stem cell-derived cardiomyocytes: boutique science or valuable arrhythmia model? **CIRC. RES.** 2013;112(6):969–976.

46. Hong JH, Choi JH, Kim TY, et al. Spiral reentry waves in confluent layer of HL-1 cardiomyocyte cell lines. **BIOCHEM. BIOPHYS. RES. COMMUN.** 2008;377(4):1269–1273.

47. Jansen JA, van Veen TAB, de Bakker JMT, et al. Cardiac connexins and impulse propagation. **J MOL CELL CARDIOL** 2010;48(1):76–82.

48. Prudat Y, Kucera JP. Nonlinear behaviour of conduction and block in cardiac tissue with heterogeneous expression of connexin 43. **J MOL CELL CARDIOL** 2014;76(C):1–9.

49. Dhillon PS, Gray R, Kojodjojo P, et al. Relationship between gap-junctional conductance and conduction velocity in mammalian myocardium. **CIRC ARRHYTHM ELECTROPHYSIOL** 2013;6(6):1208–1214.

Figures

Figure 1. Electrical activity and action potentials in SC-CMs. Sample traces of spontaneous **(A)** and triggered **(B)** action potentials (AP) by electrical pacing. **C.** Comparison of the frequency of spontaneous APs in neonatal (NCM), SC-CMs and HL-1 cardiomyocytes. Beating activity was similar in all three tested types of cardiomyocytes (the number of experiments is indicated in the bar graph). **D.** Electrical pacing of SC-CMs at different frequencies (1 and 2 Hz).

Figure 2. Characterization of voltage-dependent ion channels in SC-CMs. Shown are the stimulation protocol, sample current traces and characteristic current-voltage relationship of the fast voltage-dependent Na^+ current (I_{Na}, **A**), the T-type Ca^{2+} channel (I_{CaT}, **B**) and the L-type Ca^{2+} channel (I_{CaL}, **C**) with their respective selective inhibitors. Tetracaine (TTC, 1 mmol/L) was used to inhibit I_{Na}. The Ca^{2+} channels I_{CaT} and I_{CaL} were blocked with mibefradil (MIB, 5 µmol/L) and nifedipine (NIF, 10 µmol/L), respectively.

Figure 3. Excitation-contraction coupling in SC-CMs. A. Expression pattern of the two Ca^{2+} channels relevant for the initiation of EC-coupling: the L-type Ca^{2+} channel (Cav1.2) and the ryanodine receptor (RyR2). In addition, the protein α-actinin indicates sarcomeric orientation. **B.** Sample traces of Ca^{2+} currents elicited by a 400 ms depolarization from –40 to 0 mV (see stimulation step), line-scan images and line profiles of the Ca^{2+} transients in SC-CMs. Shown are current and Ca^{2+} traces before (black traces) and during ß-adrenergic stimulation with isoproterenol (Iso, 1 µmol/L, red traces). **C.** Quantification and statistical analysis of peak I_{CaL} and Ca^{2+} transient amplitudes, time-to-peak (TTP) and full duration at half maximum (FDHM) of the Ca^{2+} transients before (black bars) and during ß-adrenergic stimulation (grey bars), n=13-20. **D.** Functional evaluation and comparison of the SR Ca^{2+} capacity in NCM, SC-CM and HL-1 cardiomyocytes with caffeine revealed similar Ca^{2+} content in all three cell types.

Figure 4. Intercellular coupling and current-induced Ca^{2+} release in cell pairs. In the experimental setup, one cell of a cell pair is stimulated via a patch-clamp pipette to induce Ca^{2+}-induced Ca^{2+} release in *Cell 1* and in *Cell 2*. Shown are transmission light and fluorescent image of fluo-3 labeled cells, the depolarizing step from –80 to +10 mV, I_{CaL} of *Cell 1*, line-scan image and corresponding line profiles of both cells with the temporally synchronized onset of the elicited Ca^{2+} transients.

Figure 5. Metabolic coupling and dye transfer in cell pairs. A. Time series (from top left to bottom right) of dye-coupling showing dye transfer from the calcein-containing patched *Cell 1* to the neighbored *Cell 2* in a time-dependent manner. **B.** Comparison of the increase in fluorescence in *Cell 2* as a function of time in three different types of cell pairs (NCM, SC-CM and HL-1

cardiomyocyte pairs). **C.** Functional uncoupling with heptanol (1 mmol/L) leads to fast increase of fluorescence in *Cell 1*, but no dye transfer to *Cell 2*. During washout of heptanol, slow dye transfer takes place. **D.** Statistical analysis and comparison of dye transfer at 120 s between the three cell types showing significantly reduced fluorescence intensities in SC-CMs and HL-1 cells compared with NCMs (*). Reversibility of the uncoupling effect of heptanol is indicated (•). **E.** Dye-coupling in mixed cell pairs of NCMs and iPSC-CMs. Co-culture of iPSC-CMs with NCMs did not change the temporal diffusion pattern of calcein transfer. **F.** Statistical comparison of mixed cell pairs with pure NCM and iPSC-CM cultures. (NCM data in **E** and **F** are reproduced from **B** and **D**.)

Figure 6. Expression pattern of connexin-43 in different types of cardiomyocytes. A. Immunocytochemical staining of Cx43 in NCMs (**a**), ESC-CMs (**b**), HL-1 CMs (**c**) and iPSC-CMs (**d**). Arrows point towards cell-to-cell contact sites and Cx43 expression. Scale bar indicates 20 µm. **B.** Quantitative assessment of Cx43 mRNA expression by qPCR in all tested types of cardiomyocytes normalized to NCMs (n=6). Stars indicate statistical significance compared with NCMs.

Figure 7. Diffusion model of dye transfer. A. Dye transfer through gap junctions was simulated by a simple diffusion model. A semi-permeable barrier between two compartments represents the cell-to-cell contact site and diffusible particles represent the calcein molecules. Alterations of the permeability result in a change of particle diffusion into the neighbored compartment over time. **B.** Experimental data (open circles) were reproduced by this diffusion model revealing a ~6 times greater permeability in NCMs (black trace) compared with all other tested cell types (red trace). At 200 s, the difference in permeability (which is equivalent to the amount of established gap junctions between cells) resulted in a 3.7-fold greater fluorescence intensity (0.26 in NCMs compared with 0.07 in all other cardiac cell models, respectively). Experimental data are replicates of Fig. 5.

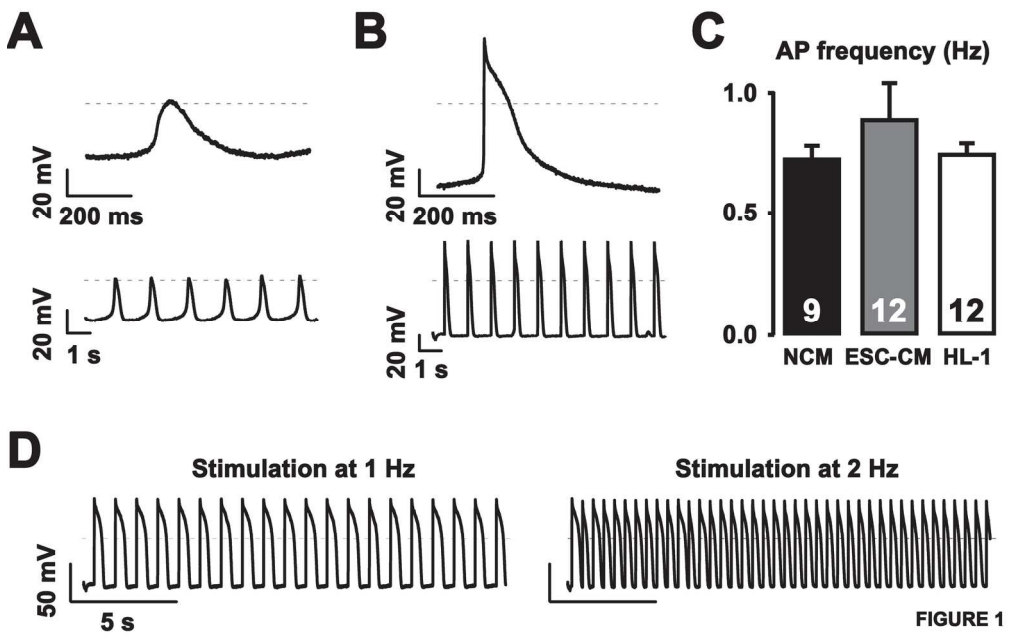

FIGURE 1

165x104mm (300 x 300 DPI)

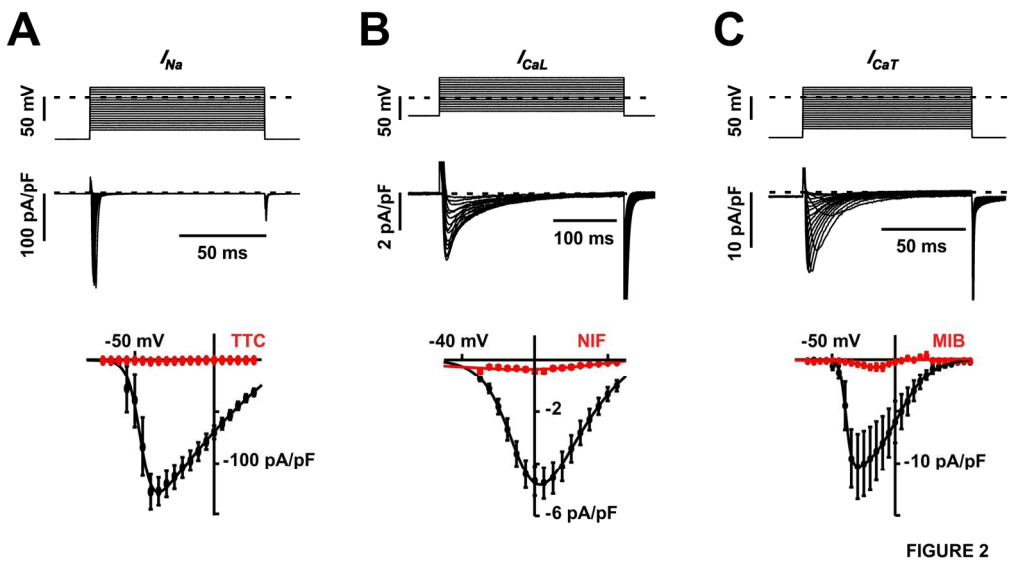

FIGURE 2

153x85mm (300 x 300 DPI)

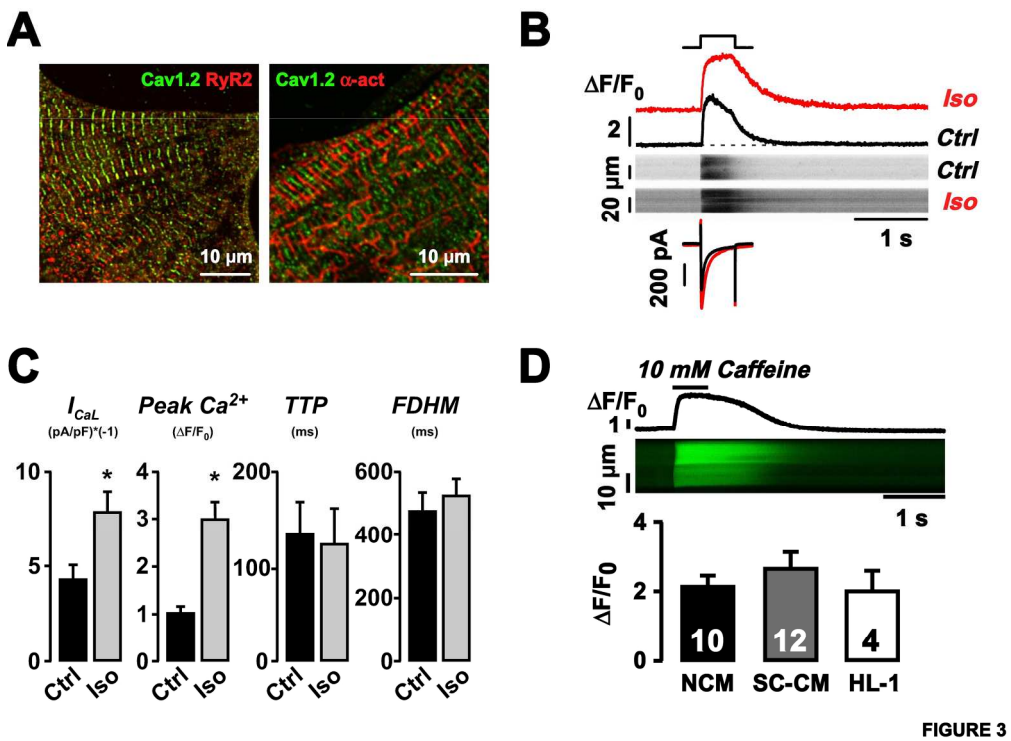

FIGURE 3

202x149mm (300 x 300 DPI)

FIGURE 4

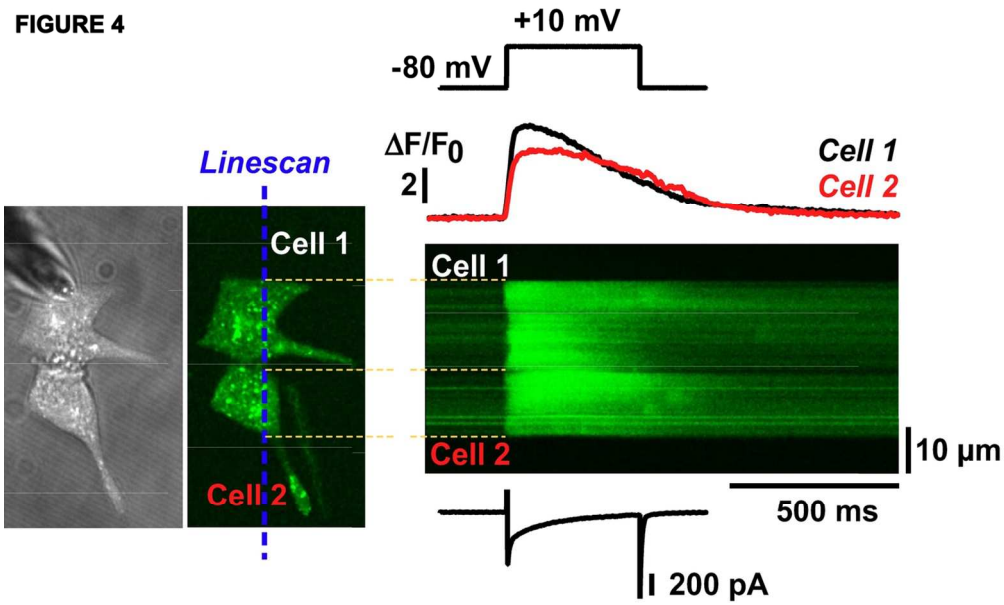

126x75mm (300 x 300 DPI)

FIGURE 5

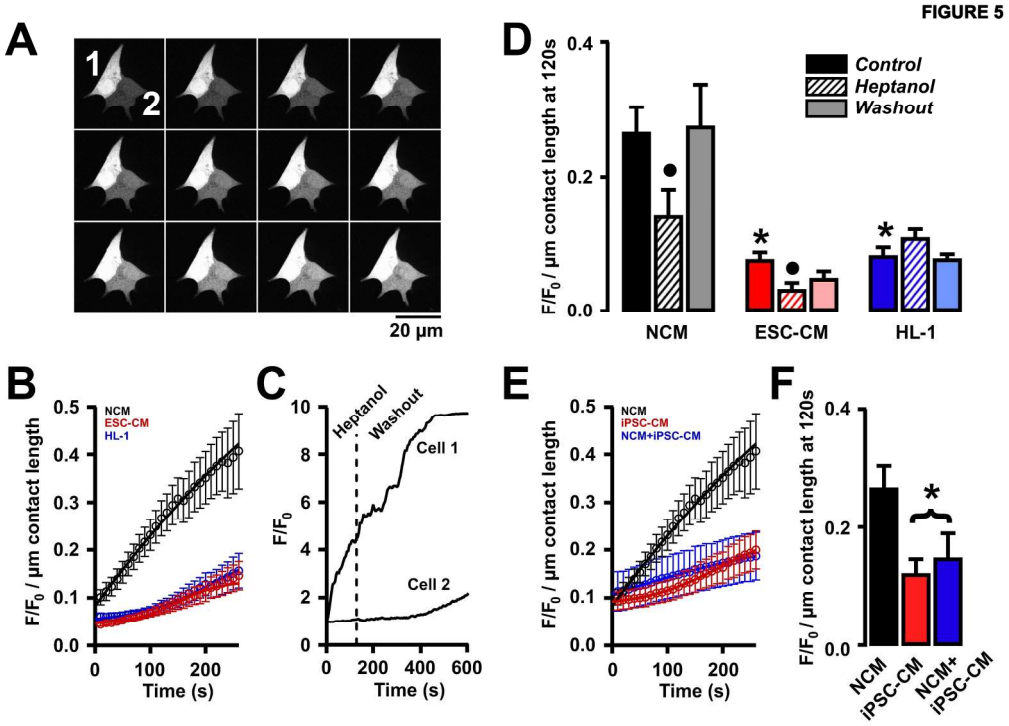

204x147mm (300 x 300 DPI)

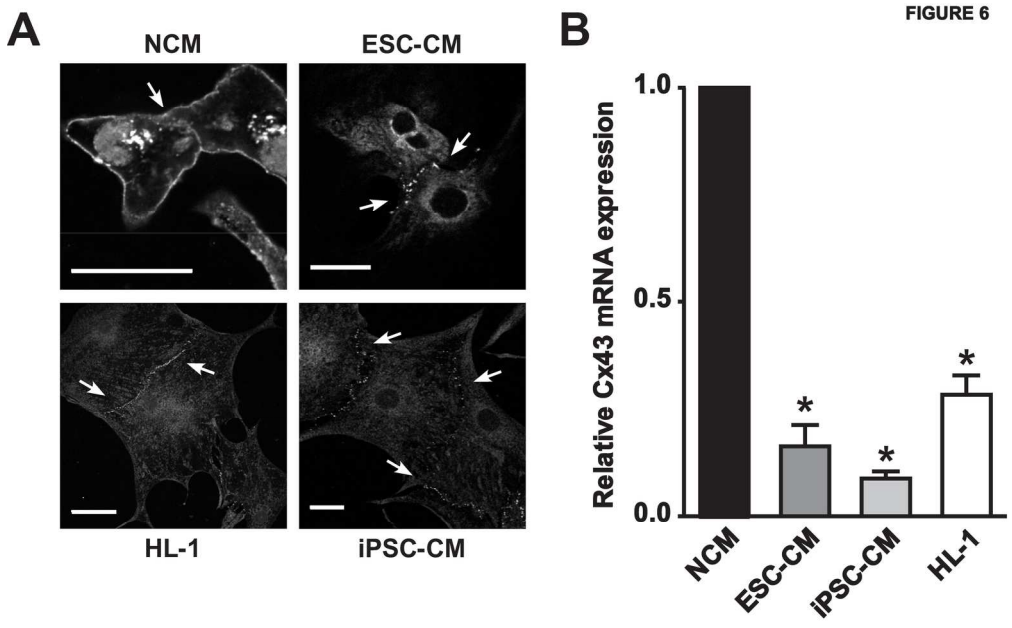

171x106mm (300 x 300 DPI)

FIGURE 7

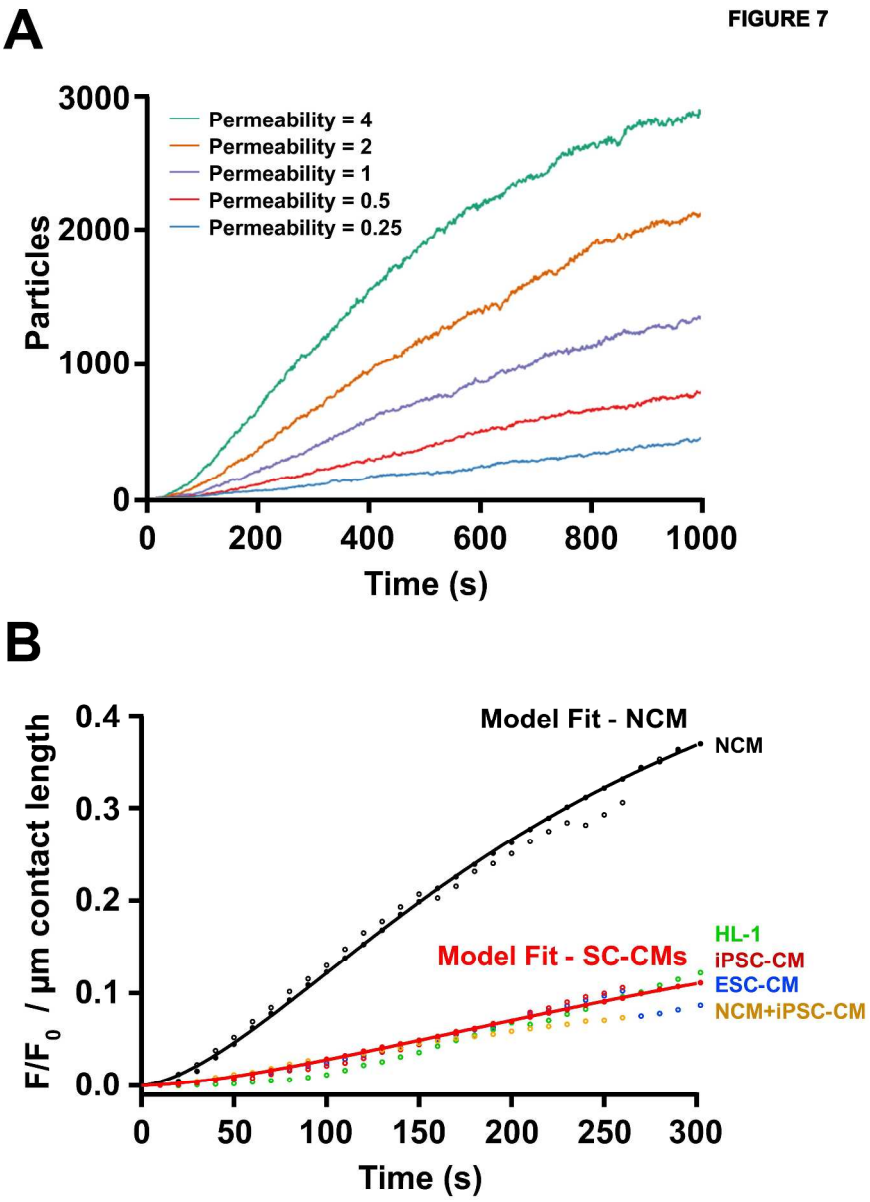

276x384mm (300 x 300 DPI)

Supplemental Information

Functional characterization and comparison of intercellular communication in stem cell-derived cardiomyocytes

Irene C. Marcu[1,2], Ardo Illaste[1], Pernilla Heuking[3], Marisa E. Jaconi[3], Nina D. Ullrich[1,2]

[1]Department of Physiology, University of Bern, Switzerland;
[2]Department of Physiology and Pathophysiology, University of Heidelberg, Germany;
[3]Department of Pathology and Immunology, University of Geneva, Switzerland.

Supplemental Material and Methods

Cardiac cell models

Differentiation of CGR8 murine embryonic stem cells was adapted from a previously described protocol using the hanging drop method [1]. Briefly, CGR8 cells were grown in Glasgow minimum essential medium (with 2 mmol/L L-Glutamine) supplemented with 10% fetal bovine serum, 0.2 mmol/L sodium pyruvate, 0.1 mmol/L non-essential amino acids, 100 U/ml penicillin and 0.1 µg/ml streptomycin (all from Invitrogen) and 50 µmol/L 2-mercaptoethanol (Sigma-Aldrich). Sub-confluent cultures (70-80% confluence) were split every 2 days using 0.25% Trypsin/EDTA (Invitrogen) and seeded at 4x1000 cells/cm² (1:10). Dishes were coated using 0.2% gelatin (Sigma-Aldrich) dissolved in phosphate buffered saline (PBS, from Invitrogen). During proliferation, spontaneous differentiation of mESCs was inhibited by 10^3 U/mL ESGRO® Supplement, which contains mouse leukemia inhibiting factor (LIF, from Millipore). Specific differentiation of mESCs into the cardiogenic lineage was achieved using the "hanging drop" method in the absence of LIF. Droplets of 20 µL containing around 500 cells were plated upside down on the inner covers of low-adhesion dishes for 2 days. Then, cell clusters were collected and kept in suspension for 4 days. The resulting embryoid bodies (EBs) were plated on gelatin-coated dishes. Spontaneous beating started at day 2 after plating. Single cells were obtained by mechanical and enzymatic dissociations: beating areas within the EBs were cut with sharp glass pipettes and digested in PBS containing 1 mg/mL of collagenase type II (Worthington) for 10 minutes at 37°C. Then cells were treated for 2-3 hours with 10 µg/mL Mitomycin C (Sigma-Aldrich) in culture medium to block proliferation of other cell types.

For comparison, murine induced pluripotent stem cell-derived cardiomyocytes (iPSC-CMs) were used. These cells are commercially available from Axiogenesis AG (Cologne, Germany). Frozen stocks of miPSC-CMs with and without GFP-label were brought into culture using Cor.At® medium according to handling instructions by Axiogenesis. Cells showed spontaneous beating activity from day 1.

For direct comparison with native cardiomyocytes, mouse neonatal ventricular cardiomyocytes (NCMs, kindly provided by Dr. Jan Kucera, University of Bern, Switzerland) were used. C57/BL6J and C57BL/6-Tg(CAG-EGFP)1Osb/J mice were obtained from the Central Animal Facility, University Hospital of Bern (originary from Charles River Laboratories). Ventricular myocytes were obtained as previously described [2]. Briefly, normal and GFP-expressing NCMs were isolated from neonatal hearts within one day after birth. Ventricles were minces and enzymatically dissociated in Ca^{2+}- and Mg^{2+}-free Hanks' balanced salt solution with penicillin/streptomycin containing 2.5% trypsin and 10 mg/L pancreatin. Fibroblast content was reduced by pre-plating cells in culture medium containing 0.1 mmol/L bromodeoxyuridine for 1-2 hours. Medium was changed every 2-3 days. The experiments were approved by the State Veterinary Office of Bern, Switzerland, according to the Swiss Federal Animal Protection Law.

Additionally, the well-characterized murine cardiac HL-1 cell line was used for our comparative experiments. Original HL-1 cells were directly obtained as a kind gift from Dr. William Claycomb [3]. Special medium (Claycomb medium, Sigma-Aldrich) was supplemented with 10% fetal bovine serum, 0.1 mmol/L norepinephrine, 1 mmol/L L-glutamine and 100 U/ml penicillin and 0.1 µg/ml streptomycin (Invitrogen). Cells were grown on 0.02% gelatin and 0.2% fibronectin (Sigma-Aldrich) coated flasks. Culture medium was changed every day, and cultures were split when full confluence was reached. All cells were kept at 37°C in a humidified incubator with 5% CO_2.

Culture of cell pairs and assessment of intercellular communication

Freshly dissociated cells were seeded at low density in order to trigger formation of cell pairs. Coupling quality was assessed in cell pairs using two experimental strategies. For electrical coupling, cells were loaded with 5 µmol/L fluo-3-AM at 37°C for 30 minutes followed by 10 minutes of de-esterification. One cell of a cell pair was patch-clamped and depolarized from -80 mV to +10 mV, triggering CICR in both cells, which was captured in line-scan images through both cells. For metabolic coupling, one cell of a cell pair was dialyzed with 5 µmol/L calcein (Molecular Probes). Full-frame images were taken every 5 seconds for a minimum period of 3 minutes. Dye coupling through gap junctions was assessed by measuring the time-dependent increase in fluorescence in the coupled cell neighbor. In order to correct for variability in dye diffusion due to different cell sizes and connecting membrane stretches, fluorescence intensities were collected in a membrane-near region of interest of constant size at the contact area in *Cell 2* of a cell pair (sparing nuclear regions) and normalized to the contact length of each cell pair. To test for gap junction-dependent dye transfer, intercellular coupling was reversibly inhibited with 1 mmol/L heptanol (Fluka). Confocal full frame and line-scan images were analyzed in ImageJ (NIH), corrected for background fluorescence and further processed using IgorPro (WaveMetrics). Normalized fluorescence is indicated as F/F_0, and relative changes in fluorescence levels are shown as $\Delta F/F_0$. All measurements were performed at constant room temperature (22°C).

Mouse primers sequences used were as follows:

GAPDH - F: TCCATGACAACTTTGGCATTG; R: CAGTCTTCTGGGTGGCAGTGA;

Cx43- F: CTGAGTGCGGTCTACACCTG; R: GAGCGAGAGACACCAAGGAC;

Cx40- F: CCACAGTCATCGGCAAGGTC; R: CTGAATGGTATCGCACCGGAA;

Cx45- F: ACCCATTTTATGTGTGCAGCA; R: GGCCTGTGACACCATACATTATC;

Cx30.2- F: TCATGCTGATCTTCCGCATCC; R: GAAGCGGTAGTGGGACACC.

Experimental solutions for electrophysiological measurements

Voltage-dependent cardiac L-type and T-type Ca^{2+} and Na^{+} currents (I_{CaL}, I_{CaT} and I_{Na}) were investigated in the whole-cell patch clamp mode. Composition of the external bath solution and internal pipette solutions required for the patch clamp experiments is summarized in **Supplemental Table 1**. The pH of the external solution was adjusted to 7.4 with NaOH, of the internal solution to pH 7.2 with CsOH (for current measurements) or KOH (for AP measurements). Internal solution was filled into patch pipettes, which were pulled from borosilicate glass micropipettes (Warner Instruments) with a horizontal puller (Zeitz Instruments) and had a resistance of 1-3 MΩ. For Ca^{2+} and Na^{+} current measurements, K^{+} channels were inhibited with 5 mM CsCl. Ca^{2+} currents were blocked with 10 µmol/L nifedipine for L-type and 5 µmol/L mibefradil for T-type Ca^{2+} channels, I_{Na} was inhibited by 1 mmol/L tetracaine. For I_{Na} measurements, external Na^{+} was reduced to 40 mmol/L NaCl, and osmolarity was compensated for using 100 mmol/L N-methyl-D-glucamin (Fluka). All chemicals were from Sigma-Aldrich, unless otherwise stated.

Supplemental Table 1: Solution composition for electrophysiological measurements using the patch clamp method. External bath solution was used as background solutions for all functional experiments.

in mmol/L	NaCl	KCl	$MgCl_2$	$CaCl_2$	HEPES	Glucose	CsAsp	KAsp	TEA-Cl	K_2-ATP	Na_2-ATP	EGTA
External bath	140	5.4	1.1	1.8	5	10	-	-	-	-	-	-
Internal (pipette)	8	-	5.9	20	20	-	120	-	20	5	-	-
Internal (for APs)	-	30	5	-	10	-	-	90	-	-	5	5

Supplemental Data

Expression pattern of cardiac connexins in ESC-, iPSC-CMs, HL-1 cells relative to NCMs

Cx43 is the predominant gap junction forming connexin in ventricular myocytes responsible for fast signal propagation across the cardiac muscle. However, three other connexins play crucial roles in cardiac conductance, namely Cx40, Cx45 and Cx30.2. Whereas Cx40 and Cx43 dominate in atrial myocytes, Cx45, the connexin with slowest conductance, governs electrical signal propagation in the sinoatrial and atrioventricular node. Cx30.2 together with Cx40 seem to modulate overall gap junction conductance in the AVN [4, 5]. mRNA expression levels of Cx43, Cx40, Cx45 and Cx30.2 were assessed in the four cell types (NCM, ESC-CMs, iPSC-CMs and HL-1 cells) using qPCR. These experiments revealed that in none of the SC-CMs, nor in HL-1 cells, the investigated connexin levels were higher than in ventricular NCMs. Since expression levels of Cx43 are highest in ventricular NCMs and it is known that all other connexins are expressed at negligible amounts in ventricular myocytes, the even lower connexin levels in SC-CMs may be considered insignificant for functional implications. In addition, one has to consider that mRNA expression levels do not directly reflect protein expression levels and channel assembly at the sarcolemma, which is usually achieved by a small fraction of gap junction proteins, while remaining connexins reside at the Golgi apparatus. Data are summarized in ***Supplemental Figure 1***. Overall statistical evaluation using one-way ANOVA revealed no significant differences among ESC-CMs, iPSC-CMs and HL-1 cells for all tested connexins. The apparently strong difference in Cx45 expression between ESC- and iPSC-CMs ($P<0.05$ from Student's t-test) may be due to the fact that ESC-derived cardiomyocytes were differently differentiated resulting in a more heterogeneous cell population with possibly higher content in pacemaker-related cardiac cells, which intrinsically express higher levels in Cx45. However, from the connexin expression pattern, we do not conclude on any specific cardiac sub-phenotype, but rather stress the difference of SC-CMs in intercellular coupling compared with native cardiomyocytes.

SUPPLEMENTAL FIGURE 1

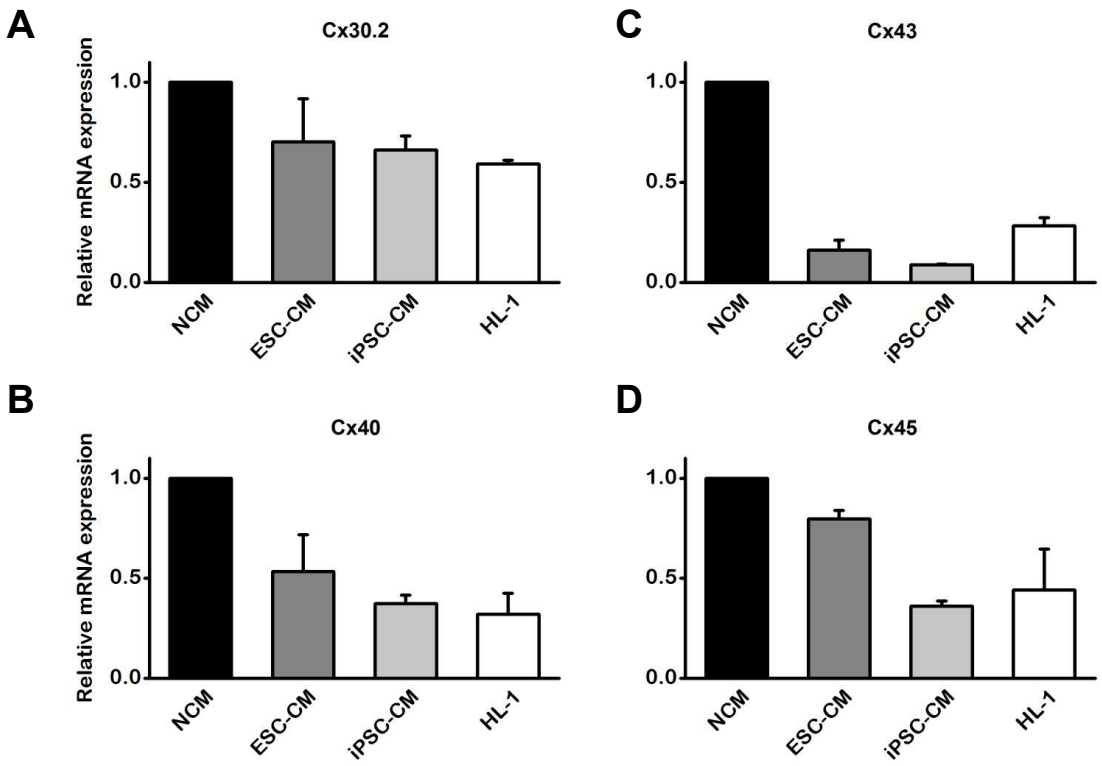

Supplemental Figure 1. Relative expression levels of cardiac-specific connexins in different types of cardiomyocytes. A. Cx30.2 expression is slightly reduced in ESC-CMs, but significantly lower in iPSC-CMs and HL-1 cells relative to NCMs. Cx40 (**B**), Cx43 (**C**) and Cx45 (**D**) levels in the three tested cells are significantly lower compared with NCMs. ANOVA tests revealed no significant differences for the individual connexins among the two SC-CM and HL-1 cell types ($P>0.05$). Cx43 data from graph **C** are reproduced from **Fig. 6** in the original manuscript.

Supplemental References

1. Meyer N, Jaconi M, Landopoulou A, et al. A fluorescent reporter gene as a marker for ventricular specification in ES-derived cardiac cells. **FEBS LETTERS** 2000;478(1-2):151–158.

2. Thomas SP, Kucera JP, Bircher-Lehmann L, et al. Impulse propagation in synthetic strands of neonatal cardiac myocytes with genetically reduced levels of connexin43. **CIRC. RES.** 2003;92(11):1209–1216.

3. Claycomb WC, Lanson NA, Stallworth BS, et al. HL-1 cells: a cardiac muscle cell line that contracts and retains phenotypic characteristics of the adult cardiomyocyte. **PROC NATL ACAD SCI USA** 1998;95(6):2979–2984.

4. Desplantez T, Dupont E, Severs NJ, et al. Gap junction channels and cardiac impulse propagation. **J. MEMBR. BIOL.** 2007;218(1-3):13–28.

5. Jansen JA, van Veen TAB, de Bakker JMT, et al. Cardiac connexins and impulse propagation. **J MOL CELL CARDIOL** 2010;48(1):76–82.